Skewness of the elliptic flow distribution in $\sqrt{s_{NN}} = 5.02$ TeV PbPb collisions from the HYDJET + + model

P. Cirkovic,[1] J. Milosevic,[1,2,*] L. Nadderd,[1] F. Wang,[3,4] and X. Zhu[3]

[1]*Vinča Institute of Nuclear Sciences, University of Belgrade, Mike Petrovića Alasa 12-14, Vinca 11351, Belgrade, Serbia*

[2]*University of Oslo, Department of Physics, Oslo, Blindern N-0316, Norway*

[3]*College of Science, Huzhou University, Huzhou, Zhejiang 313000, People's Republic of China*

[4]*Department of Physics and Astronomy, Purdue University, Indiana 47907, USA*

(Received 4 July 2019; accepted 24 February 2020; published 12 March 2020)

The elliptic flow (v_2) event-by-event fluctuations in PbPb collisions at 5.02 TeV are analyzed within the HYDJET + + model. Using the multiparticle, so-called Q-cumulant method, $v_2\{2\}$, $v_2\{4\}$, $v_2\{6\}$, and $v_2\{8\}$ are calculated and used to study their ratios and to construct skewness ($\gamma_1^{\rm exp}$) as a measure of the asymmetry of the elliptic flow distribution. Additionally, in order to check if there is a hydrodynamics nature in the elliptic collectivity generated by the HYDJET + + model, the ratio of $v_2\{6\} - v_2\{8\}$ and $v_2\{4\} - v_2\{6\}$ distributions is calculated. The analysis is performed as a function of the collision centrality. In order to check the HYDJET + + model responses, the results of this analysis are compared to the corresponding experimental measurements from the ALICE, ATLAS, and CMS experiments. A rather good qualitative agreement is found.

DOI: 10.1103/PhysRevC.101.034907

I. INTRODUCTION

In ultrarelativistic nucleus-nucleus collisions sufficiently high energy densities have been achieved that a new state of matter, the quark-gluon-plasma (QGP) has been created. The QGP created in these collisions exhibits a collective expansion which could be described by relativistic hydrodynamic flows. The collectivity in the QGP has been studied in experiments at the Relativistic Heavy Ion Collider (RHIC) [1–3] and the Large Hadron Collider (LHC) [4–15]. The geometry of the overlap interaction zone in nucleus-nucleus collisions is anisotropic. This anisotropy is converted into momentum space by the hydrodynamic expansion. The momentum anisotropy can be characterized by a Fourier expansion of the emitted hadron yield distribution in azimuthal angle, ϕ [16–18]:

$$\frac{dN}{d\phi} \propto 1 + 2\sum_n v_n \cos[n(\phi - \Phi_n)], \tag{1}$$

where Fourier coefficients, v_n, represent magnitude of the azimuthal anisotropy measured with respect to the corresponding flow symmetry plane angle, Φ_n. The flow symmetry plane is determined by the geometry of the participant nucleons and can be reconstructed from the emitted particles themselves. Because of fluctuations in the initial spatial geometry, all orders of Fourier harmonics are present. The second-order Fourier coefficient, v_2, is called elliptic flow, while the angle Φ_2 corresponds to the flow symmetry plane which is determined by the beam direction and the shorter axis of the roughly lenticular shape of the nuclear overlap region.

Another experimental method to determine the v_n coefficients is multiparticle cumulant analysis which uses the Q-cumulant method [19]. The multiparticle cumulant technique has the advantage of suppressing short-range correlations arising from jets and resonance decays and revealing the collective nature of the observed azimuthal correlations. The two-, four-, six-, and eight-particle azimuthal correlations are calculated as

$$\begin{aligned}
\langle\langle 2\rangle\rangle &= \langle\langle e^{in(\phi_1-\phi_2)}\rangle\rangle,\\
\langle\langle 4\rangle\rangle &= \langle\langle e^{in(\phi_1+\phi_2-\phi_3-\phi_4)}\rangle\rangle,\\
\langle\langle 6\rangle\rangle &= \langle\langle e^{in(\phi_1+\phi_2+\phi_3-\phi_4-\phi_5-\phi_6)}\rangle\rangle,\\
\langle\langle 8\rangle\rangle &= \langle\langle e^{in(\phi_1+\phi_2+\phi_3+\phi_4-\phi_5-\phi_6-\phi_7-\phi_8)}\rangle\rangle,
\end{aligned} \tag{2}$$

where $\langle\langle\cdots\rangle\rangle$ denotes averaging over all particle multiplets and over all events from a given centrality class,[1] n is harmonic order and ϕ_i ($i = 1, \ldots, 8$) are the azimuthal angles of particles from a given particle multiplet. The corresponding

*Corresponding author: Jovan.Milosevic@cern.ch

[1]Each centrality class is determined by a given range in $b/2R$, where R is the radius of the Pb nucleus and $\vec{b}$ is the impact parameter vector connecting centers of the colliding nuclei in the plane perpendicular to the beam axis. The value of b is distributed according to b^2. The centrality is given as a fraction of the total inelastic PbPb cross section, with 0% denoting the most central collisions.

multiparticle cumulants $c_n\{2k\}$ $(k = 1, \ldots, 4)$ are then given as [19]

$$\begin{aligned} c_n\{2\} &= \langle\langle 2\rangle\rangle, \\ c_n\{4\} &= \langle\langle 4\rangle\rangle - 2\langle\langle 2\rangle\rangle^2, \\ c_n\{6\} &= \langle\langle 6\rangle\rangle - 9\langle\langle 4\rangle\rangle\langle\langle 2\rangle\rangle + 12\langle\langle 2\rangle\rangle^3, \\ c_n\{8\} &= \langle\langle 8\rangle\rangle - 16\langle\langle 2\rangle\rangle\langle\langle 6\rangle\rangle - 18\langle\langle 4\rangle\rangle^2 \\ &\quad + 144\langle\langle 4\rangle\rangle\langle\langle 2\rangle\rangle^2 - 144\langle\langle 2\rangle\rangle^4. \end{aligned} \tag{3}$$

Finally, the Fourier coefficients v_n are connected to the above defined multiparticle cumulants through the following relations:

$$\begin{aligned} v_n\{2\} &= \sqrt{c_n\{2\}}, \\ v_n\{4\} &= \sqrt[4]{-c_n\{4\}}, \\ v_n\{6\} &= \sqrt[6]{\frac{1}{4}c_n\{6\}}, \\ v_n\{8\} &= \sqrt[8]{-\frac{1}{33}c_n\{8\}}. \end{aligned} \tag{4}$$

The unitless standardized skewness, $\gamma_1^{\rm exp}$, of the event-by-event elliptic flow magnitude distribution is a measure of the asymmetry about its mean. This standardized skewness can be estimated using the cumulant elliptic flow harmonics defined as in Ref. [20]:

$$\gamma_1^{\rm exp} = -6\sqrt{2}v_2\{4\}^2\frac{v_2\{4\} - v_2\{6\}}{(v_2\{2\}^2 - v_2\{4\}^2)^{3/2}}. \tag{5}$$

In the case where the event-by-event elliptic flow magnitude fluctuations stem from an isotropic Gaussian transverse initial-state energy density profile, the skewness $\gamma_1^{\rm exp}$ becomes equal to zero. But, non-Gaussian fluctuations in the initial-state energy density profile could be present [20], and as a consequence will produce differences in the higher order cumulant $v_2\{2k\}$ $(k \geqslant 2)$ coefficients. As Eq. (5) is an approximation of the standardised skewness γ_1 defined in [20], it is possible to test its validity through the universal equality given in [20]:

$$v_2\{6\} - v_2\{8\} = \tfrac{1}{11}(v_2\{4\} - v_2\{6\}). \tag{6}$$

Equation (6) is a consequence of the fine splitting and ordering between the higher order cumulants $v_2\{2k\}$ $(k \geqslant 2)$ which, within a pure hydrodynamics, appears due to the skewness of the fluctuations of the elliptic flow (see Eq. (12) in [20] and the discussion there).

In this paper, we study the skewness of the elliptic flow distribution using the HYDJET++ model. The basic features of HYDJET++ model [21] are described in Sec. II. Using HYDJET++ model, approximately 6×10^7 PbPb collisions at $\sqrt{s_{NN}} = 5.02$ TeV are simulated and analyzed. The obtained results together with the corresponding experimental results [10,22,23] and discussions are given in Sec. III. The results are presented over a wide range of centralities going from central (5–10% centrality) up to rather peripheral (55–60% centrality) PbPb collisions. The analyzed p_T interval is restricted to the $0.3 \leqslant p_T \leqslant 3$ GeV/c range where hydrodynamics dominates, while the η range covers the $(-1.0, 1.0)$ region. A summary is given in Sec. IV.

II. HYDJET++

In the Monte Carlo HYDJET++ model, relativistic heavy ion collisions are simulated. The HYDJET++ model consists of two components which simulate soft and hard processes. The hydrodynamical evolution of the system is provided by the soft part of the model, while the hard part describes multiparton fragmentation within the formed medium. Within the hard part, jet quenching effects are also taken into account. The minimal transverse momentum $p_T^{\rm min} = 10.0$ GeV/c of hard scattering of an incoming parton regulates whether it contributes to the soft or to the hard part. The partons which are produced with $p_T < p_T^{\rm min}$, or which are quenched below $p_T^{\rm min}$ do not contribute to the hard part. The hard part of the HYDJET++ model consists of PYTHIA [24] and PYQUEN [25] models. These models simulate initial parton-parton collisions, radiative energy loss of partons, and parton hadronization.

In order to significantly decrease the time needed to generate a HYDJET++ event, the soft part is represented with a thermal state generated on the chemical and thermal freeze-out hypersurfaces which are obtained from the parametrization of the relativistic ideal hydrodynamics with preset freeze-out conditions using the FASTMC generator [26]. The hydrodynamic expansion of the formed system suddenly ends at a given chemical temperature (T^{ch}), but the system expands further and breaks down at thermal freeze-out temperature (T^{th}). The temperature at thermal freeze-out is set to 0.105 GeV, while the proper time is set to 13.2 fm/c. The value of chemical freeze-out temperature is set to 0.165 GeV. All chemical potentials are set to zero.

In the HYDJET++ simulation, the elliptic modulation of the final freeze-out hypersurface is given by the spatial eccentricity $\epsilon(b) = \frac{R_y^2(b) - R_x^2(b)}{R_y^2(b) + R_x^2(b)}$, where b is the collision impact parameter. The azimuthal angle of the cell velocity vector ϕ_u is not necessarily identical to the position azimuthal angle of the cell ϕ from the freeze-out hypersurfaces. They are connected through the modulation of the flow velocity profile $\delta(b)$ [26] as

$$\tan\phi_u = \sqrt{\frac{1 - \delta(b)}{1 + \delta(b)}}\tan\phi. \tag{7}$$

In the HYDJET++ model, the $\delta(b)$ is obtained via the following parametrization [21]:

$$\begin{aligned} \delta(b) &= \frac{\sqrt{1 + 4B[\epsilon(b) + B]} - 1}{2B} \\ B &= C[1 - \epsilon^2(b)]\epsilon(b), \end{aligned} \tag{8}$$

where $\epsilon(b)$ is simply parameterized as $\epsilon(b) = k\epsilon_0$, with ϵ_0 given by $\epsilon_0 = b/2R$ (R is the radius of the colliding nuclei in symmetric AA collisions). Here, C and k are centrality-independent coefficients. They are obtained from the best fit of the CMS data and their values are $C = 5.6$ and $k = 0.101$. Within the hydrodynamical approach [21,27], the magnitude

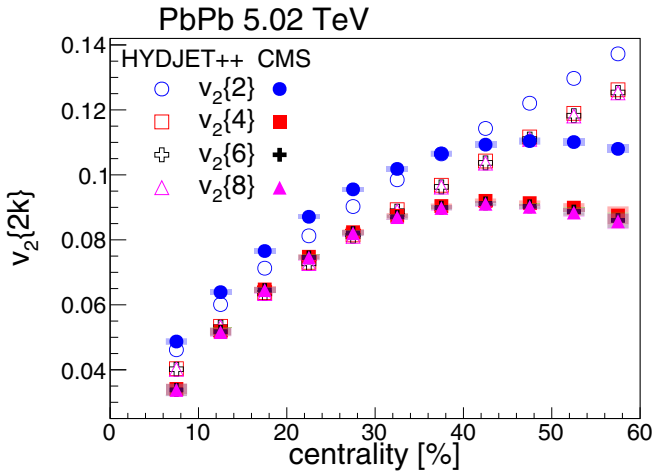

FIG. 1. Elliptic flow harmonics of different cumulant orders $v_2\{2k\}$ $(k = 1, \ldots, 4)$ in PbPb collisions at $\sqrt{s_{NN}} = 5.02$ TeV from the HYDJET + + model and the experimental CMS data [23] are shown with open and closed symbols as a function of the collision centrality. Data cover the $0.3 < p_T < 3.0$ GeV/c and $|\eta| < 1.0$ range. The shadow boxes represent the systematic uncertainties of the experimental results, while the statistical uncertainties are smaller than the symbol size.

of the elliptic flow is regulated by the corresponding $\epsilon(b)$ and by $\delta(b)$ as

$$v_2 \propto \frac{2[\delta(b) - \epsilon(b)]}{[1 - \delta^2(b)][1 - \epsilon^2(b)]}. \tag{9}$$

In the HYDJET + + model, the fluctuations are introduced through the multiplicity fluctuations. Flow fluctuations are additionally enhanced by smearing of ϵ and δ parameters [28,29].

The details of the model can be found in the HYDJET + + manual [21].

III. RESULTS

The centrality dependence of the elliptic flow harmonics obtained from different cumulant orders $v_n\{2k\}$ $(k = 1, \ldots, 4)$ extracted from PbPb collisions generated by the HYDJET + + model at 5.02 TeV incident energy are shown as open symbols in Fig. 1. In order to compare these results with the experimental ones, in the same figure are also shown corresponding CMS results taken from [23]. For each centrality interval, ranged from the central 5–10% to rather peripheral 55–60%, a cumulant analysis is performed within $0.3 < p_T < 3.0$ GeV/c and $|\eta| < 1.0$.

Both theoretical and experimental results exhibit a characteristic ordering between cumulants of different order: $v_2\{2\} > v_2\{4\} \approx v_2\{6\} \approx v_2\{8\}$ for all centralities. The difference between the $v_2\{2\}$ and higher order cumulants is more pronounced in the experimental data than in the HYDJET + + predictions. Qualitatively, the HYDJET + + model properly predicts centrality dependence of $v_2\{2k\}$, up to centrality of 35%. A relatively good agreement between the HYDJET + + predictions and the experimental data is achieved for more central and semicentral collisions where the relative difference goes from 5% to 10%. The discrepancy between the experimental data and model prediction becomes very pronounced going to more peripheral collisions. While the experimental $v_2\{2k\}$ values saturate, the model prediction of the $v_2\{2k\}$ values continues to increase.

Because in Fig. 1 the rank ordering between the higher order cumulants is not very visible, in Fig. 2 the centrality dependencies of the ratios of the elliptic flow coefficients are shown for different cumulant orders. Because for all centrality regions the ratios are smaller then 1, they indicate the following rank ordering: $v_2\{4\} > v_2\{6\} > v_2\{8\}$. This confirms inconsistency with a pure Gaussian fluctuations model of the v_2 harmonics. The differences are smaller than 1% and slightly increase going from central to peripheral collisions. In the same figure are shown CMS experimental results taken from [23]. In contrast to the HYDJET + + predictions, the experimentally measured ratios show much stronger centrality dependence, and the deviation from unity reaches even a few percent in most peripheral events. A relatively good agreement between the experimental data and HYDJET + + predictions exists only for rather central events (up to 40% centrality) and especially for the $v_2\{8\}/v_2\{6\}$ ratio. For collisions with centralities above 40%, the relative difference between $v_2\{4\}$ and $v_2\{6\}$ or $v_2\{8\}$ in the experimental data is larger than in the model, causing a stronger deviation from unity and thus a stronger centrality dependence. This may suggest a larger deviation from Gaussian v_2 fluctuations in the data than simulated by the HYDJET + + model.

Figure 3 shows $(v_2\{4\} - v_2\{6\})$ divided with 11 and $v_2\{6\} - v_2\{8\}$ quantities as a function of centrality in PbPb collisions at $\sqrt{s_{NN}} = 5.02$ TeV simulated with the HYDJET + + model and measured by ALICE [22]. The quantities extracted from the experimental data are observed to be in agreement, which demonstrates the validity of Eq. (6). The corresponding quantities extracted from the HYDJET + + simulation are observed to be not only in a mutual agreement but also in agreement with the experimentally measured ones.

In order to check a hydrodynamic behavior of the medium simulated with the HYDJET + + model, in Fig. 4 is plotted the ratio $(v_2\{6\} - v_2\{8\})/(v_2\{4\} - v_2\{6\})$ for PbPb collisions at $\sqrt{s_{NN}} = 5.02$ TeV. According to Eq. (6), in an ideal hydrodynamic behavior with a finite v_2 skewness one could expect that the plotted ratio should be equal to $\frac{1}{11} \approx 0.091$. The HYDJET + + model predicts an increase of that ratio going from central to peripheral collisions. It has the smallest value and is closest to the theoretical prediction value of about 0.11 at the most central 5–10% analyzed collisions, and increases up to the value of 0.14 for the most peripheral collisions. The mean value of this ratio over the 5–60% centrality range is 0.127 ± 0.002, and is in an agreement with the experimental CMS and ALICE results of 0.18 ± 0.08 [30] and 0.11 ± 0.05 [31] respectively.[2]

[2]Statistical and systematical uncertainties of the ratios from the CMS and ALICE data are too big to be plotted. It would be valuable to have better statistics in the future.

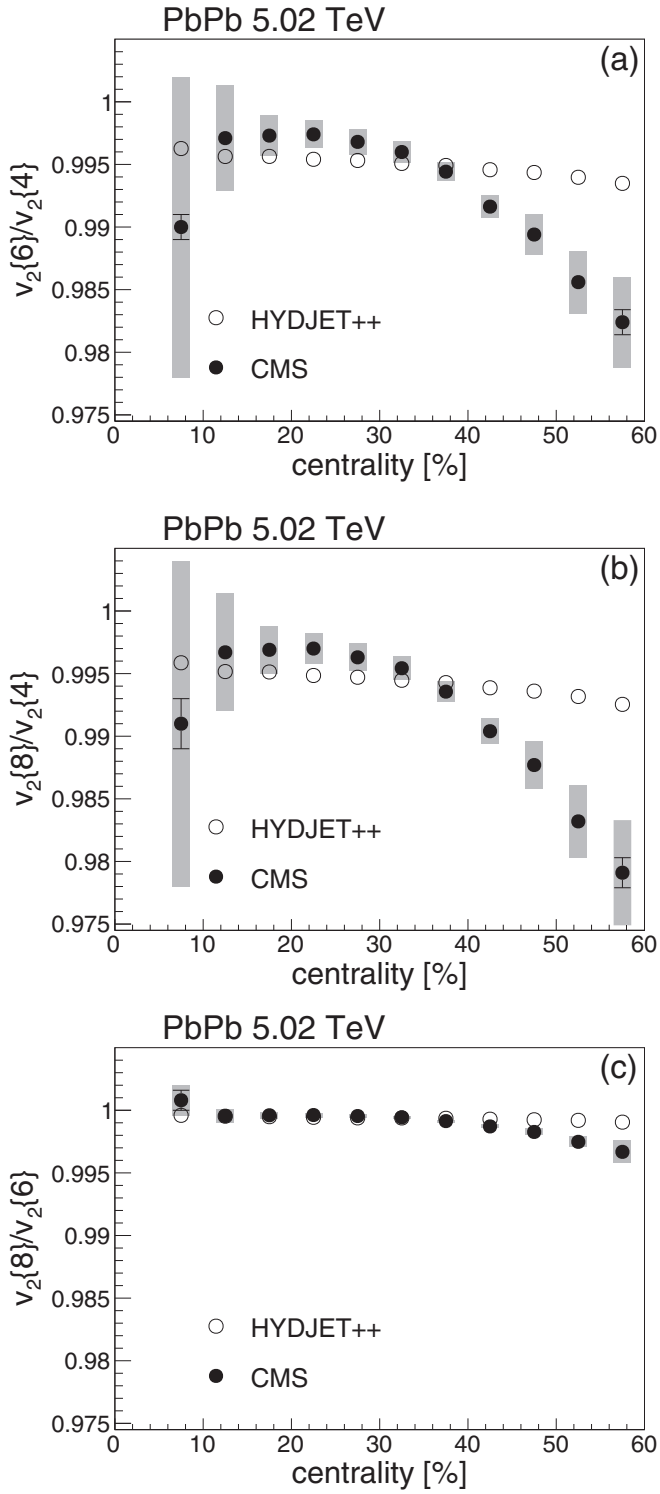

FIG. 2. Centrality dependencies of the ratios of higher order elliptic flow cumulants: $v_2\{6\}/v_2\{4\}$ (top), $v_2\{8\}/v_2\{4\}$ (middle), and $v_2\{8\}/v_2\{6\}$ (bottom) in PbPb collisions at $\sqrt{s_{NN}} = 5.02$ TeV. The HYDJET++ model predictions are shown with open symbols, while the experimental CMS data [23] are shown with closed symbols. Data cover the $0.3 < p_T < 3.0\,\mathrm{GeV}/c$ and $|\eta| < 1.0$ range. The error bars represent the statistical uncertainties. The shadow boxes represent the systematic uncertainties of the experimental results.

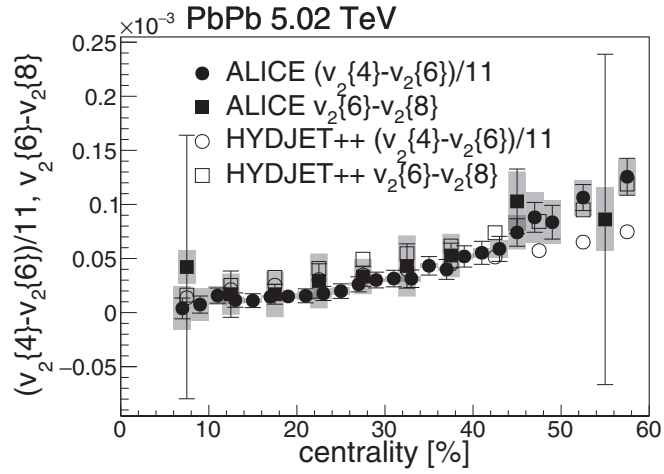

FIG. 3. Centrality dependence of the differences of the v_2 Fourier harmonic calculated from different multiparticle cumulants in PbPb collisions from the HYDJET++ model and from the ALICE [22] experimental data at $\sqrt{s_{NN}} = 5.02$ TeV. The error bars represent the statistical uncertainties. The shadow boxes represent the systematic uncertainties of the experimental results.

Figure 5 depicts centrality dependence of the elliptic flow skewness γ_1^{exp} calculated using different cumulant orders by Eq. (5) in PbPb collisions at $\sqrt{s_{NN}} = 5.02$ TeV simulated by the HYDJET++ model. In the same figure, the HYDJET ++ model prediction is compared with the experimental CMS and ATLAS results. Differently from the HYDJET++ prediction and the CMS results, the ATLAS results are obtained within the $p_T > 0.5\,\mathrm{GeV}/c$ and $|\eta| < 2.5$ range from PbPb collisions at $\sqrt{s_{NN}} = 2.76$ TeV. The CMS results are taken from [23], while the ATLAS results are reconstructed based on data taken

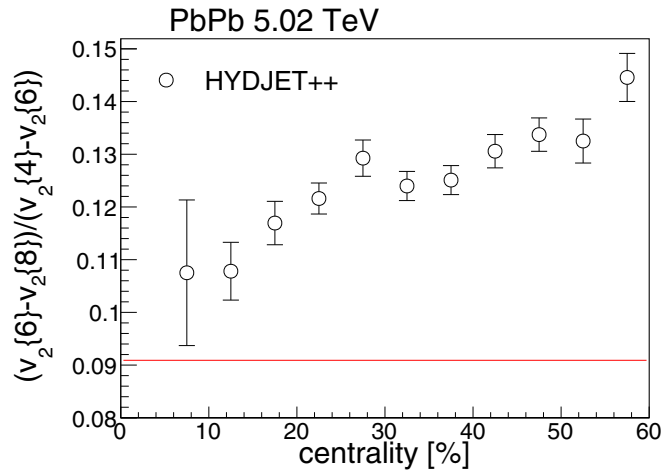

FIG. 4. The centrality dependence of the ratio $(v_2\{6\} - v_2\{8\})/(v_2\{4\} - v_2\{6\})$ extracted from PbPb collisions simulated with the HYDJET++ model at $\sqrt{s_{NN}} = 5.02$ TeV. The red horizontal line indicates the theoretical prediction of $\frac{1}{11} \approx 0.091$. The analysis is performed for the $0.3 < p_T < 3.0$ GeV/c and $|\eta| < 1.0$ range. The error bars represent the statistical uncertainties.

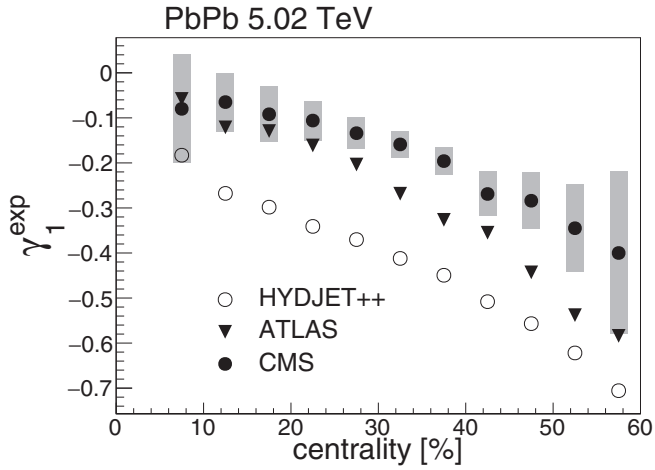

FIG. 5. The centrality dependence of the skewness calculated from the v_2 values of different cumulant orders in PbPb collisions at $\sqrt{s_{NN}} = 5.02$ TeV. Open symbols show the HYDJET + + model prediction, while closed circles show the CMS experimental result (taken from [23]). The analyses for HYDJET + + and CMS are performed for the $0.3 < p_T < 3.0$ GeV/c and $|\eta| < 1.0$ range. Also depicted in closed triangles are the ATLAS experimental results for PbPb collisions at $\sqrt{s_{NN}} = 2.76$ TeV for the $p_T > 3.0$ GeV/c and $|\eta| < 2.5$ range. The ATLAS results are recalculated from data taken from [10,32]. The shadow boxes represent the systematic uncertainties of the experimental results, while the statistical uncertainties are smaller than the symbol size.

from [10,32]. Finite values for the skewness are observed for the HYDJET + + model simulations and for the experimental data. The shape of the centrality dependence of $\gamma_1^{\rm exp}$ from the HYDJET + + model is qualitatively similar to those found from the experimental data, but the magnitudes of $\gamma_1^{\rm exp}$ differ significantly. While both experimental measurements of $\gamma_1^{\rm exp}$ are in a quantitative agreement with the theoretical predictions from [20], the HYDJET + + model gives a stronger $\gamma_1^{\rm exp}$ deviation from zero. In collisions with centrality below 35% this is because the $(v_2\{2\} - v_2\{4\})$ value in the HYDJET + + model, presumably due to insufficient fluctuations [28,29], is significantly smaller than those in the experimental data [see Eq. (5)]. In collisions with centrality above 35% the main contribution of the difference comes from the significantly larger $v_2\{4\}$ from the model than from the data. The experimental CMS [23], ATLAS [10,32], and ALICE [22] results for $v_2\{4\}$ are in a fair mutual agreement. These differences of the HYDJET + + model from experimental data are worth exploring in future studies.

IV. CONCLUSIONS

The cumulant analysis method for the v_2 elliptic flow coefficients in PbPb collisions generated by the HYDJET + + model at $\sqrt{s_{NN}} = 5.02$ TeV shows that the event-by-event fluctuations in the v_2 magnitude are not Gaussian. The analysis is performed as a function of centrality, covering the range from 5% up to 60% collision centralities. As expected, the $v_2\{2\}$ clearly has a magnitude larger than the ones from the higher order cumulants. But, a rank ordering between the higher order cumulants, $v_2\{4\} > v_2\{6\} > v_2\{8\}$, with differences smaller than 1%, is also observed. Comparison of the $(v_2\{4\} - v_2\{6\})/11$ and $v_2\{6\} - v_2\{8\}$ distributions shows that the HYDJET + + predictions are in a good agreement with the ALICE data [22]. A hydrodynamic check for the centrality dependence of the ratio $(v_2\{6\} - v_2\{8\})/(v_2\{4\} - v_2\{6\})$ shows that the HYDJET + + model gives an increasing distribution with the mean value close to the expectation from ideal hydrodynamics, similarly to what is observed in the experimental CMS [30] and ALICE [31] data. In the case where there is a difference in the magnitudes from the higher order cumulants, the skewness $\gamma_1^{\rm exp}$ is found to be negative with an increasing magnitude as collisions become less central. The HYDJET + + model qualitatively predicts a correct behavior of the centrality dependence of the skewness, but the magnitude of $\gamma_1^{\rm exp}$ is larger than for the experimental data.

ACKNOWLEDGMENTS

The authors acknowledge support of the Bilateral Cooperation between the Republic of Serbia and the People's Republic of China 451-03-478/2018-09/04 "Phenomenology in high energy physics." Support from the Ministry of Education Science and Technological Development, Republic of Serbia (Grant No. 171019), National Natural Science Foundation of China (Grant No. 11847315), and the U.S. Department of Energy (Grant No. DE-SC0012910) is also acknowledged.

[1] B. B. Back *et al.* (PHOBOS Collaboration), Phys. Rev. Lett. **89**, 222301 (2002).
[2] K. H. Ackermann *et al.* (STAR Collaboration), Phys. Rev. Lett. **86**, 402 (2001).
[3] K. Adcox *et al.* (PHENIX Collaboration), Phys. Rev. Lett. **89**, 212301 (2002).
[4] K. Aamodt *et al.* (ALICE Collaboration), Phys. Rev. Lett. **105**, 252302 (2010).
[5] K. Aamodt *et al.* (ALICE Collaboration), Phys. Rev. Lett. **107**, 032301 (2011).
[6] B. B. Abelev *et al.* (ALICE Collaboration), J. High Energy Phys. 06 (2015) 190.
[7] J. Adam *et al.* (ALICE Collaboration), Phys. Rev. Lett. **116**, 132302 (2016).
[8] G. Aad *et al.* (ATLAS Collaboration), Phys. Lett. B **707**, 330 (2012).
[9] G. Aad *et al.* (ATLAS Collaboration), Phys. Rev. C **86**, 014907 (2012).
[10] G. Aad *et al.* (ATLAS Collaboration), J. High Energy Phys. 11 (2013) 183.
[11] S. Chatrchyan *et al.* (CMS Collaboration), Eur. Phys. J. C **72**, 2012 (2012).
[12] S. Chatrchyan *et al.* (CMS Collaboration), Phys. Rev. C **87**, 014902 (2013).

[13] S. Chatrchyan *et al.* (CMS Collaboration), Phys. Rev. C **89**, 044906 (2014).
[14] S. Chatrchyan *et al.* (CMS Collaboration), J. High Energy Phys. 02 (2014) 088.
[15] V. Khachatryan *et al.* (CMS Collaboration), Phys. Rev. C **92**, 034911 (2015).
[16] J.-Y. Ollitrault, Phys. Rev. D **48**, 1132 (1993).
[17] S. Voloshin and Y. Zhang, Z. Phys. C **70**, 665 (1996).
[18] A. M. Poskanzer and S. A. Voloshin, Phys. Rev. C **58**, 1671 (1998).
[19] A. Bilandzic, R. Snellings, and S. Voloshin, Phys. Rev. C **83**, 044913 (2011).
[20] G. Giacalone, L. Yan, J. Noronha-Hostler, and J.-Y. Ollitrault, Phys. Rev. C **95**, 014913 (2017).
[21] I. P. Lokhtin, L. V. Malinina, S. V. Petrushanko, A. M. Snigirev, I. Arsene, and K. Tywoniuk, Comput. Phys. Commun. **180**, 779 (2009).
[22] S. Acharya *et al.* (ALICE Collaboration), J. High Energy Phys. 07 (2018) 103.
[23] A. Sirunyan *et al.* (CMS Collaboration), Phys. Lett. B **789**, 643 (2019).
[24] T. Sjostrand, S. Mrenna, and P. Skands, J. High Energy Phys. 05 (2006) 026.
[25] I. P. Lokhtin and A. M. Snigirev, Eur. Phys. J. C **45**, 211 (2006).
[26] N. S. Amelin, R. Lednicky, I. P. Lokhtin, L. V. Malinina, A. M. Snigirev, Iu. A. Karpenko, Yu. M. Sinyukov, I. Arsene, and L. Bravina, Phys. Rev. C **77**, 014903 (2008).
[27] U. A. Wiedemann, Phys. Rev. C **57**, 266 (1998).
[28] L. V. Bravina, B. H. Brusheim Johansson, G. Kh. Eyyubova, V. L. Korotkikh, I. P. Lokhtin, L. V. Malinina, S. V. Petrushanko, A. M. Snigirev, and E. E. Zabrodin, Eur. Phys. J. C **74**, 2807 (2014).
[29] L. V. Bravina, E. S. Fotina, V. L. Korotkikh, I. P. Lokhtin, L. V. Malinina, E. N. Nazarova, S. V. Petrushanko, A. M. Snigirev and E. E Zabrodin, EPJ Web Conf. **126**, 04006 (2016).
[30] https://www.hepdata.net/record/80151
[31] https://www.hepdata.net/record/ins1666817
[32] https://www.hepdata.net/record/ins1233359